

Real-Time Simulation of Static VAR Compensator and Static Synchronous Compensator



Anjali A. Bhandakkar, Lini Mathew

Abstract: In recent years, deregulation, open access, and co-generation in electrical power system are creating transmission voltage sags, swells, forced outages, and frequently followed by black-outs, congestion scenario, and many such problems. Reactive power limit is one of the major causes of voltage instability in the power system, and improving the system's reactive power handling capacity via Flexible AC transmission System (FACTS) devices is one of the remedies for prevention of voltage instability. The typical representatives of parallel FACTS devices for its avoidance are Static Synchronous Compensator (STATCOM) and Static VAR Compensator (SVC). Real-Time Simulator facilitates a physically large and spatially diverse or distributed power system to be accurately simulated in laboratory, and physical devices, like controllers or protection equipment can be tested in real time, even with introduction of faults, overloads, loss of generation condition, and with many more conditions for stability analysis purpose. This paper presents comparison of power flow parameter and the performance characteristic of the controllers on Real-Time Simulator OPAL-RT-OP4510 with SVC, and STATCOM. The waveforms of voltage, current, active and reactive power during the Real-Time execution are taken from the simulation environment to the outside world, using input/output devices, and seen on Digital Storage Oscilloscope (DSO). The validation is done on multi-machine-9-bus system. The results of Real-Time Simulation during LLLG fault indicate that STATCOM supplies reactive power independent of line voltage, whereas SVC behaves as constant susceptance when the reactive power required by the system is above its rated capacity. The power flow parameters with both the controllers are comparable during steady state operation.

Keywords: DSO, FACTS, LFA, LLLG Fault, Real-Time Simulator.

I. INTRODUCTION

The power sector is in its fast growing phase to meet the growing demand for electricity. With the integration of Distributed Energy Resources (DER) in the Distribution

Network (DN), the conventional network has upgraded from a passive network to an active network. With high penetration of DER, the network experiences high R/X ratios, unpredicted variation of source, and in addition to the continuously variation of loads. With all these challenges, power grid is committed to provide good quality power to the consumers and maintain the stability of the network. Load flow studies is a tool, to analyze the network, and for taking suitable control measures in case of necessity [1]. Real-Time Simulators have been used extensively in the planning and design of electrical systems since last three decades. It has vital significance in Power system and power electronics based projects [2]. The evolution of simulation tools has been possible due to the rapid evolution of high-speed computing technologies, at an affordable cost, also with auto-code generation for application in industrial controllers [3]. Dynamic Reactive Power Compensation for voltage support using SVC, has been done in Power System Simulator for Engineers (PSS/E) to predict the performance of the SVC [4]. The improvement in the voltage stability of the grid, with the wind farm using Doubly Fed Induction Generator (DFIG) connection, was proposed with SVC with an Adaptive Neuro Fuzzy Inference System (ANFIS) controller, and tested using MATLAB [5]. The transient stability of wind farm, with Fixed Speed Induction Generators (FSIGs) using Static Synchronous Compensator (STATCOM) and SVCs has been carried out using Simulink. [6]. A hybrid topology consisting SVC in series with a STATCOM with significantly lower rating was put in shunt to the point of common coupling (PCC), such that the STATCOM was rated for just 15% of the total compensation and the SVC was rated for the rest of the 85%, thus providing a lower cost solution for applications in HV and EHV systems with the control to provide a constant reactive current support irrespective of the drop in grid voltage. Simulations were performed in EMTDC/PSCAD platform [7]. The functioning of the STATCOM using simulink platform and its capabilities for reactive power compensation and fast response were discussed in [8]. An extensive review of recent trends in application of Real-Time simulations with FACTS devices was discussed in [9]. Since most of the research is done on MATLAB/Simulink, EMTDC, PSCAD software, author is encouraged to work on Real-Time Simulator to check the performance of SVC.

Section II details power flow parameters computation of an uncompensated system and with SVC, and STATCOM.

Manuscript received on February 10, 2020.

Revised Manuscript received on February 20, 2020.

Manuscript published on March 30, 2020.

* Correspondence Author

Anjali A. Bhandakkar*, Electrical Engineering Department, National Institute of Technical Teacher's Training and Research, Chandigarh, Chandigarh, India, Email: bhandakkar13@gmail.com

Lini Mathew, Electrical Engineering Department, National Institute of Technical Teacher's Training and Research, Chandigarh, Chandigarh, India, Email: lenimathew@yahoo.com

© The Authors. Published by Blue Eyes Intelligence Engineering and Sciences Publication (BEIESP). This is an open access article under the CC BY-NC-ND license (<http://creativecommons.org/licenses/by-nc-nd/4.0/>)

Section III describes the Real Time Simulation of SVC, and STATCOM on OP4510. Section IV is about results obtained by .m-file, and V, I, active and reactive power waveforms with SVC, and STATCOM executed on real-time simulator. Section V is about the conclusion.

II. LFA COMPUTATION

In the recent years, several high-level scientific languages, such as Mathematica, Matlab, and Modelica, have become popular for both research and educational purposes, computing good results in the field of power system analysis [10]. However, MATLAB proved to be the best user’s choice as it processes the matrix-oriented programming, and has excellent plotting proficiencies and Simulink, a graphical environment which highly simplifies design of control scheme. The schematic representation of power system is shown in Fig. 1, consisting generation, load, and transmission lines connecting the buses.

A. LFA of an uncompensated System

The schematic representation of power system is shown in Fig. 1, consisting generation, load, and transmission lines connecting the buses.

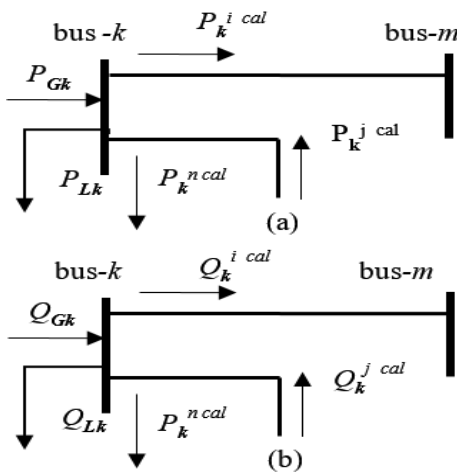


Fig. 1. Power balance at bus-k (a) Active power (b) Reactive power

For the steady-state operation of a power system, the ‘mismatch power equations’ expressing active power and reactive power generation, load, and power exchanged through the transmission elements connecting to the buses must add up to zero. The active and reactive power at bus-k are given by (1), (2).

$$P_{Gk} - P_{Lk} - \sum_{i=1}^n P_k^{i cal} = 0 \tag{1}$$

$$Q_{Gk} - Q_{Lk} - \sum_{i=1}^n Q_k^{i cal} = 0 \tag{2}$$

P_{Gk} , P_{Lk} are real power generation, and load, and Q_{Gk} , Q_{Lk} are reactive power generation, and load connected to bus-k respectively. $P_k^{i cal}$, $Q_k^{i cal}$ are real and reactive power exchanged by bus-k with bus-i of the network, and given by

$$(3) \quad \text{and} \tag{4}$$

$$P_k^{i cal} = \sum_{i=1}^n V_k^2 G_{kk} + V_k V_i [G_{ki} \cos(\theta_k - \theta_i) + B_{ki} \sin(\theta_k - \theta_i)] \tag{3}$$

$$Q_k^{i cal} = \sum_{i=1}^n -V_k^2 B_{kk} + V_k V_i [G_{ki} \sin(\theta_k - \theta_i) - B_{ki} \cos(\theta_k - \theta_i)] \tag{4}$$

The per unit values of transmission parameters, voltage, generations and loads are used for LF computation [11]. Newton Raphson (NR) Algorithm is very popular due to its fast convergence with a less number of iterations as compared to the other methods such as Gauss-Seidel method, Decoupled method and Fast decoupled method.

B. LFA with SVC

The basic configuration of SVC, connected via a coupling transformer, to the main AC supply bus, is shown in Fig. 2. It comprises one or more banks of fixed or switched shunt capacitors or reactors, Thyristor Switched Capacitors (TSC), Thyristor Controlled Reactors (TCR), and harmonic filter/s. With proper coordination of the capacitor switching, and reactor control, the VAR output can be varied continuously between its capacitive and inductive ratings. It generates as well as absorbs reactive power as per system voltage. Thus SVC is a static compensator and controls the voltage of power system with variation in its reactive output current [12].

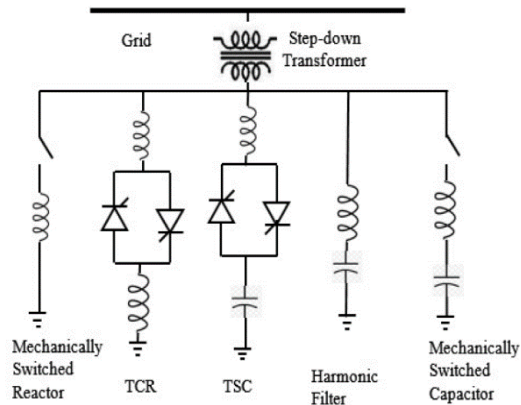


Fig. 2. Basic configuration of SVC

The SVC can be seen as an adjustable reactance with either firing-angle limits or reactance limits, as shown in Fig.3.

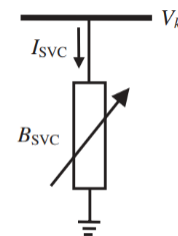


Fig. 3. Power flow model of SVC

With reference to Fig. 3, current drawn by the SVC, $I_{SVC} = jB_{SVC} V_k$ and the reactive power injected at bus-k, is

$$Q_{SVC} = Q_k = -V_k^2 B_{SVC} \quad (6)$$

The linearized equation is given by (7).

$$\begin{bmatrix} \Delta P_k \\ \Delta Q_k \end{bmatrix}^{(i)} = \begin{bmatrix} 0 & 0 \\ 0 & Q_k \end{bmatrix}^{(i)} \begin{bmatrix} \Delta \theta_k \\ \Delta B_{SVC} / B_{SVC} \end{bmatrix} \quad (7)$$

B_{SVC} is taken to be the state variable and is updated after each iteration as per (8).

$$B_{SVC}^{(i)} = B_{SVC}^{(i-1)} + \left(\frac{\Delta B_{SVC}}{B_{SVC}} \right)^{(i)} \times B_{SVC}^{(i-1)} \quad (8)$$

Thus the SVC susceptance, jB_{SVC} , required to maintain the nodal voltage magnitude at the specified value is computed [13].

C. LFA with STATCOM

STATCOM, a VSC based FACTS device generates synchronous voltage of fundamental frequency, with controllable magnitude and phase angle. It is shunt-connected to a system via a coupling transformer as shown in Fig. 4 (a), and can inject or absorb reactive power to or from the bus to which it is connected and thus regulate the bus voltage magnitude. This STATCOM model is known as Power Injection Model (PIM) or Voltage Source Model (VSM). The bus at which the STATCOM is connected is represented as a PV bus, which may change to a PQ bus in the event of limits being violated.

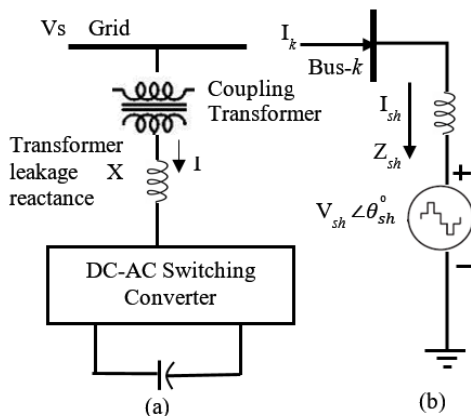


Fig. 4. STATCOM (a) Basic configuration (b) Power flow model

The maximum capacitive or inductive output current supplied by STATCOM is independent of the ac system voltage, and can be operated even at 0.2 per unit system voltage level [14]. It is represented as a voltage source behind the reactance as shown in Fig. 4(b). Assuming the conductance of STATCOM as zero, the active and reactive power injection at bus- k is given by (10), (11).

$$P_k = V_k^2 G_{sh} + V_k V_{sh} [G_{sh} \cos(\theta_k - \theta_{sh}) + B_{sh} \sin(\theta_k - \theta_{sh})] \quad (10)$$

$$Q_k = -V_k^2 B_{sh} + V_k V_{sh} [G_{sh} \sin(\theta_k - \theta_{sh}) - B_{sh} \cos(\theta_k - \theta_{sh})] \quad (11)$$

The output power of STATCOM is given by (12), (13).

$$P_{sh} = V_{sh}^2 G_{sh} + V_{sh} V_k [G_{sh} \cos(\theta_{sh} - \theta_k) + B_{sh} \sin(\theta_{sh} - \theta_k)] \quad (12)$$

$$Q_{sh} = -V_{sh}^2 B_{sh} + V_{sh} V_k [G_{sh} \sin(\theta_{sh} - \theta_k) - B_{sh} \cos(\theta_{sh} - \theta_k)] \quad (13)$$

With the power equations (12), and (13), and the linearized STATCOM model voltage magnitude V_{sh} and phase angle θ_{sh} as the state variables, Jacobian (14) can be constructed to solve for mismatch equations [15].

$$\begin{bmatrix} \Delta P_k \\ \Delta Q_k \\ \Delta P_{sh} \\ \Delta Q_{sh} \end{bmatrix} = \begin{bmatrix} \frac{\partial P_k}{\partial \theta_k} & \frac{\partial P_k}{\partial V_k} V_k & \frac{\partial P_k}{\partial \theta_{sh}} & \frac{\partial P_k}{\partial V_{sh}} V_{sh} \\ \frac{\partial Q_k}{\partial \theta_k} & \frac{\partial Q_k}{\partial V_k} V_k & \frac{\partial Q_k}{\partial \theta_{sh}} & \frac{\partial Q_k}{\partial V_{sh}} V_{sh} \\ \frac{\partial P_{sh}}{\partial \theta_k} & \frac{\partial P_{sh}}{\partial V_k} V_k & \frac{\partial P_{sh}}{\partial \theta_{sh}} & \frac{\partial P_{sh}}{\partial V_{sh}} V_{sh} \\ \frac{\partial Q_{sh}}{\partial \theta_k} & \frac{\partial Q_{sh}}{\partial V_k} V_k & \frac{\partial Q_{sh}}{\partial \theta_{sh}} & \frac{\partial Q_{sh}}{\partial V_{sh}} V_{sh} \end{bmatrix} \begin{bmatrix} \Delta \theta_k \\ \Delta V_k \\ \Delta \theta_{sh} \\ \Delta V_{sh} \end{bmatrix} \quad (14)$$

III. REAL TIME SIMULATION

The Real-Time Simulator OPAL-RT-OP4510 has 4 cores. RT-LAB system is it's one of the features. The RT-LAB system architecture consists a host computer and a target computer connected by TCP/IP. RT-LAB is a distributed real-time platform that allows users to test dynamical models built in MATLAB/Simulink environment, for Hardware in Loop (HIL) simulation at very high accuracy, low cost, and in real time. It also has special Simulink-based modelling tools, namely, ARTEMiS and RT-Events which allow real time simulation in multi-core processors, which is required for very complex non-linear systems like power system in real time, with high precision and high stability. ARTEMiS is a power system real-time solver that provides a high degree of stability for the discrete time state-space models. It enables parallel computation of electric circuits on different CPU cores. It also enables to simulate a very large number of switches in real-time. It facilitates to gain important computational time when compared to SimPowerSystems because it makes full pre-computation of all state-space equations before the real-time loop. RT-Events block-set lead to accurate simulation because RT-Events blocks propagate zero crossing information at fixed time step, and the Time Stamped Bridge use this information to produce compensated output voltages to the load. For executing the model on OPAL-RT, the MATLAB Simulink model is be divided into a number of subsystems, and can be run in multi core/processors in parallel without affecting the dynamics of the original system. In the RT-LAB model, there is always one master subsystem, and the console subsystem, however, slave subsystem is only needed when the model is too large and complex, for distributing the computational effort across multiple cores. The signal communication is done across the subsystems with the help of OpCom block. For connecting two subsystems ARTEMiS transmission lines/distributed parameter lines are generally used. The steps to simulate the system in RT-LAB are as follows.

- Starting compilation
- Separating RT-LAB model
- Generating C code
- Using System Target File (TLC file) : rtlab_rtmodel.tlc
 - Using Template Make file (TMF file) : rtlab_rtmodel.tmf
- Transferring the generated C code
- Building the generated C code
- Transferring the built model
- Loading the model
- Executing model
- Reset

The host computer facilitates the edition of Simulink model, model compilation with RT-LAB and user interface. On the target computer, the real-time model gets executed and with the input-output ports, the controlling signals can be communicated to the real-time hardware. FTP and TELNET communication is possible with the host. The Real Time Simulator does the real-time model execution. It has REDHAT as an operating system. Table 1 gives the specifications of OPAL-RT OP4510 Simulator [15].

Table- I: Specifications of OPAL-RT OP4510 Simulator

SN	Particular	Specification
1	Model OP4510	Propagation delay of digital input-output as 40ns
2	CPU	4 Cores
3	Processor	Xeon E3 3.2 GHz
4	FPGA	Kintex-7 XILINX Board
5	Hard disk	128 GB
6	6 optical link	50 Mbps
7	Analog in	16 channels
8	Analog out	16 channels
9	Digital in	32 channels
10	Digital out	32 channels
11	Encoder, decoder, input / output expansion boards and other applications	12RS422

parameters mentioned to actual MATLAB/Simulink model of the multi-machine-9-bus system is developed by converting per unit values of all the parameters to actual values, by taking base of 100 MVA (S_b) and 230 kV (V_b). SVC connected on bus-8 is developed. The model is made compatible for execution on OPAL-RT OP4510 Simulator. The Top-level model consists two sub-systems, master subsystem, and console subsystem, as shown in Fig.5. The Console Subsystem (SC_VIEW) consists control over the variation of the type of fault and location of fault, and the scopes to see the response of network, as shown in Fig.6. The Master Subsystem, (SM_GRID), consisting of multi-machine-9-bus network, the fault subsystem, the OPAL-RT OpComm block, input/output blocks OpControl, Analog in, and Analog out, as shown in Fig. 7.

Similarly MATLAB model with shunt connected STATCOM at the same location, and compatible for execution on OPAL-RT OP4510 Simulator is also developed.

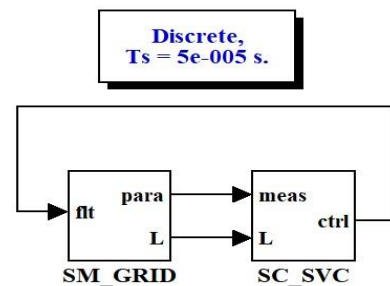


Fig. 5. Top Level model of SVC

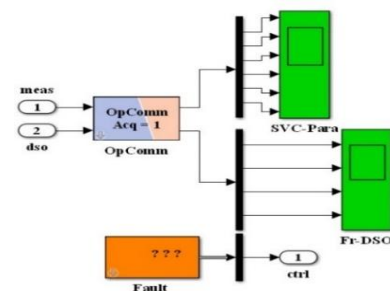


Fig. 6. Console sub-system model of SVC

MATLAB/Simulink model of the multi-machine-9-bus system is developed by converting per unit values of all the

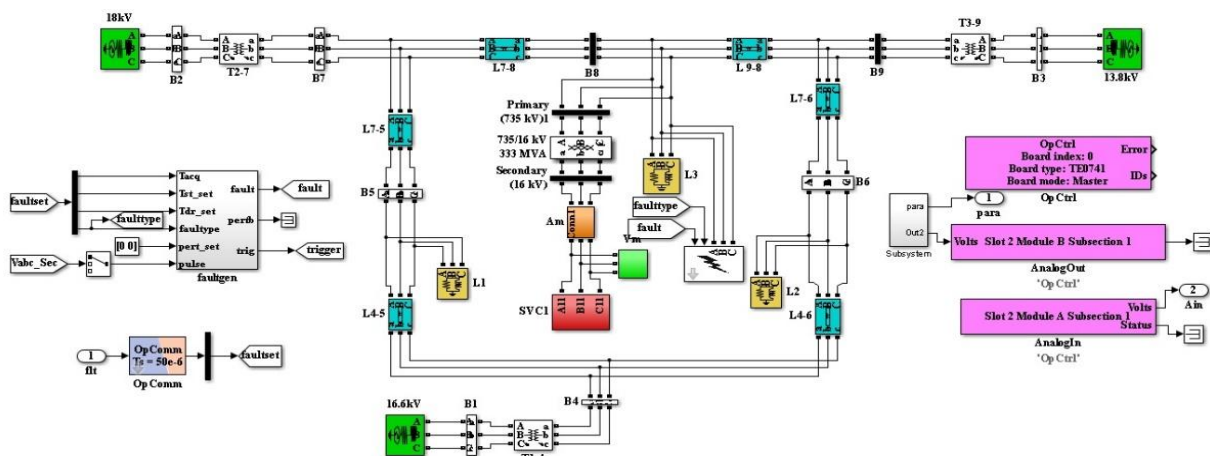


Fig. 7. Master sub-system model of SVC

IV. RESULT AND DISCUSSION

The LFA of the multi-machine-9-bus system without and with SVC and STATCOM is computed. MATLAB .m-file is developed, based on Newton Raphson (NR) Algorithm as it is very popular due to its fast convergence with a less number of iterations as compared to the other methods such as Gauss-Seidel method, Decoupled method and Fast decoupled method. The multi-machine-9-bus system consists of 9 lines, 3 generators connected to bus-1, bus- 2, and bus-3 through a step-up transformer, 3-loads connected to bus-5, bus-6, and bus-8 as shown in Fig.8.

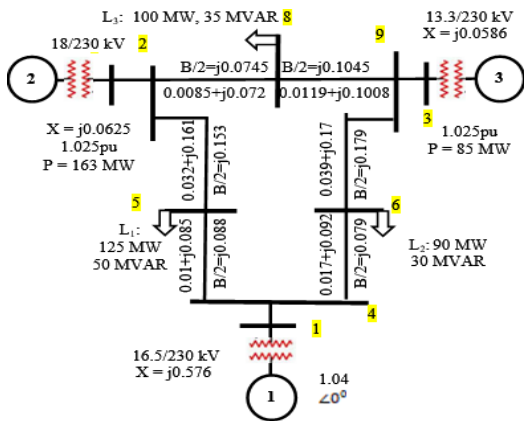


Fig. 8. Multi-machine 9 bus system

A. LFA Computation Results

The MATLAB .m-file is developed for power flow parameter computation of multi-machine 9 bus system, and with SVC, and STATCOM, and the results are given in Table II.

Table-II: LFA of an uncompensated system, with SVC and STATCOM

Bus	Para	Uncomp	SVC	STATCOM
1	V ∠θ	1.040∠0	1.04∠0	1.04 ∠0.0
	P ± j Q	71.641 +27.046j	71.641 +17.289j	71.5355 +16.2709j
2	V ∠θ	1.025 ∠9.28	1.025 ∠9.28	1.0250 ∠9.2497
	P ± j Q	163.0 +6.654j	163.0 +0.768	163.0 +0.1538j
3	V ∠θ	1.025 ∠4.665	1.025 ∠4.67	1.0250 ∠4.6905
	P ± j Q	85.0 -10.86j	85.0 -13.708j	85.0 -14.0055j
4	V ∠θ	1.026 ∠-2.217	1.031 ∠-2.22	1.0317 ∠-2.2007
	P ± j Q	0.0 +0.0j	0.0 +0.0j	0.0 +0.0j
5	V ∠θ	0.996 ∠-3.989	1.010 ∠-4.0	1.0115 ∠-3.9898
	P ± j Q	-125.0 -50.0j	-125.0 -33.915j	-125.0 -32.2080j
6	V ∠θ	1.013 ∠-3.687	1.017 ∠-3.69	1.0174 ∠-3.6476
	P ± j Q	-90.0 -30.0j	-90.0 -30.0j	-90.0 -30.0j
7	V ∠θ	1.026 ∠3.72	1.029 ∠3.72	1.0297 ∠3.7107
	P ± j Q	0.0+0.0j	0.0+0.0j	0.0 +0.0j
8	V ∠θ	1.016 ∠0.728	1.019 ∠0.73	1.0190 ∠0.7493
	P ± j Q	-100.0 -35.0j	-100.0 -35.0j	-100.0 -35.0j

9	V ∠θ	1.032 ∠1.967	1.034 ∠1.967	1.0341 ∠1.9972
	P ± j Q	0.0+0.0j	0.0+0.0j	0.0+0.0j

The total real power loss occurring in the system without SVC, and STATCOM is 4.641 MW and the reactive power loss is -94.5624 MVAR.

The LFA computation shows, total real power loss occurring with SVC in the system is 4.5627 MW and -j92.1689 MVAR. The required susceptance of SVC for injecting reactive power to maintain bus voltage of 1.01 per unit at bus-5 is $B_{SVC} = 0.1577$ pu, and SVC has injected reactive power in the network of magnitude $Q_{SVC} = -16.085$ MVAR.

The LFA computation shows, real power loss occurring with STATCOM in the system is 4.5355 MW and the reactive power loss is -94.7888 MVAR. The output voltage of STATCOM is 1.0291 pu, and injected reactive power of -18.10 MVAR, to maintain bus voltage of 1.0115 per unit at bus-5. Due to the reactive power injection by SVC, and STATCOM, the reactive power generation, and reactive power flow through the system have further reduced with STATCOM, as compared to with SVC and without the controllers.

Fig.9 shows the bar chart representation for comparing bus voltage magnitude with and without the controllers. It clearly indicates that, with implementation of SVC at bus-5, the voltage magnitude of bus-5 has improved, along with improvement of voltage magnitude at all the buses. The bus voltage angle and real power at the bus is nearly same.

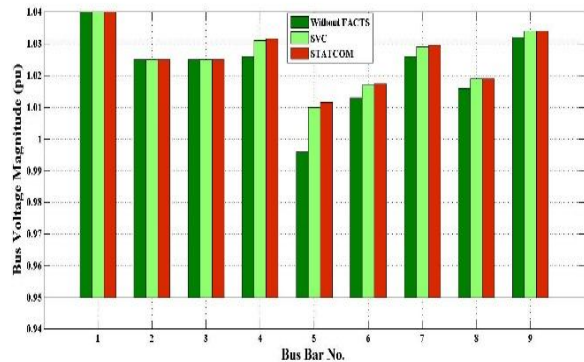


Fig. 9. Bus Voltage Magnitude at various buses of an Uncompensated system and with SVC and STATCOM

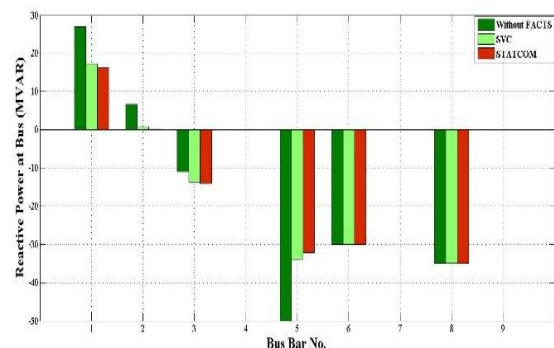


Fig. 10. Reactive Power at various buses of an Uncompensated system and with SVC and STATCOM

Fig.10 shows the bar chart representation for comparing reactive power at the various bus. The reactive power generation by generator-1, and generator-2, has reduced. At bus-5, SVC injects a reactive power of 16.085 MVAR, in addition to the reactive power flow supply of 33.915 MVAR, to meet the total load of 50 MVAR. At bus-4, bus-7, and bus-9, reactive load is zero, and at bus-6 and bus-8, connected reactive load demand is met.

B. Real-Time execution of SVC, and STATCOM

The MATLAB/Simulink models developed for the three cases were made compatible with the OPAL-RT OP4510 Real-Time Simulator. Fig. 11 shows the waveforms of the models without any compensating devices. The voltage, current, active and reactive power within the rated value during the healthy condition, but as the LLLG fault is introduced, voltage drops to a very low value (approximately zero), with sudden increase in current, and reduced active and reactive power. Fig.12 shows 5 different waveforms, I, Q, V, Firing angle of TCR, and number of TSC in operation with SVC connected in the system. Each waveform is divided in 5 parts A, B, C, D, and E. As shown in Fig.12, from the initial point up to point 'A', SVC is in floating condition, by switching TSC-1 on, 5th waveform and TCR almost at full conduction (alpha=96 degrees) as shown in 4th waveform. In the 3rd waveform, at point 'A', system voltage is suddenly increased to 1.025 pu, the SVC acts in inductive mode, absorbs reactive power (Q = -95 MVAR), as shown in 2nd waveform, by switching TCR at full conduction (alpha = 96 degrees), and disconnecting all TSCs. At point 'B', the voltage is suddenly lowered to 0.93 pu, all the three TSCs are switched in sequentially, as shown on 5th waveform, and the TCR absorbs nominal reactive power (alpha =120 degrees). Each time a TSC is switched on, the TCR alpha angle changes suddenly from 180 degrees (no conduction) to 90 degrees (full conduction). At point 'C', as the system voltage is increased to 1.0 pu, SVC is again in floating condition. Thus SVC absorbs reactive power with increase in grid voltage and maintains the nodal voltage, and injects reactive power with decrease in grid voltage and maintains the nodal voltage. Thus

SVC maintains the nodal voltage, when there is small variation in system voltage, if injection/absorption of reactive power by SVC is within its rated value. At point 'D', LLLG fault is introduced on load-3, connected to bus-8, resulting an abrupt increase in current, as seen in 1st waveform, followed by drop in line voltage to 0.1 pu as seen in 2nd waveform. In such case, SVC is unable to supply reactive power, required to raise the system voltage to 1.0 pu, as seen in 3rd waveform. It behaves as a constant susceptance when the reactive power requirement exceeds its MVAR rating. This is the major drawback of SVC, that it is unable to supply reactive power, when it is needed the most. At point 'E', the fault is cleared and system voltage is regulated to the reference value.

The waveforms shown in Fig.13, are of STATCOM in voltage control mode. A controlled voltage source is used to bring about the changes in system voltage. Initially the reference voltage of STATCOM is set to 1.0 pu, hence it is in floating condition, (zero current exchange). With sudden increase in voltage to 1.025, STATCOM absorbs reactive power, with the reduction in DC voltage. With the reduction in source voltage 0.97, it supplies reactive power, with increase in DC capacitor voltage. Since the waveforms are taken with actual magnitude of parameters, the variation in voltage magnitude has to be carefully observed in the initial part of waveform. When the source voltage set back to its nominal value, the STATCOM operates in floating state. With the introduction of LLLG fault, the system voltage reduces approximately to zero, the STATCOM supplies capacitive reactive power, to maintain the system voltage. Thus the output power of STATCOM is independent of system voltage. Since STATCOM has to supply the power during the fault, its voltage must be higher than the system voltage, which necessitates increased capacitor voltage. The variation in reactive power output of STATCOM is accompanied by variation in the DC voltage. There is a small phase angle shift (0.5 degrees) of STATCOM output voltage with the line voltage, required to maintain a small active power flow compensating transformer and converter losses.

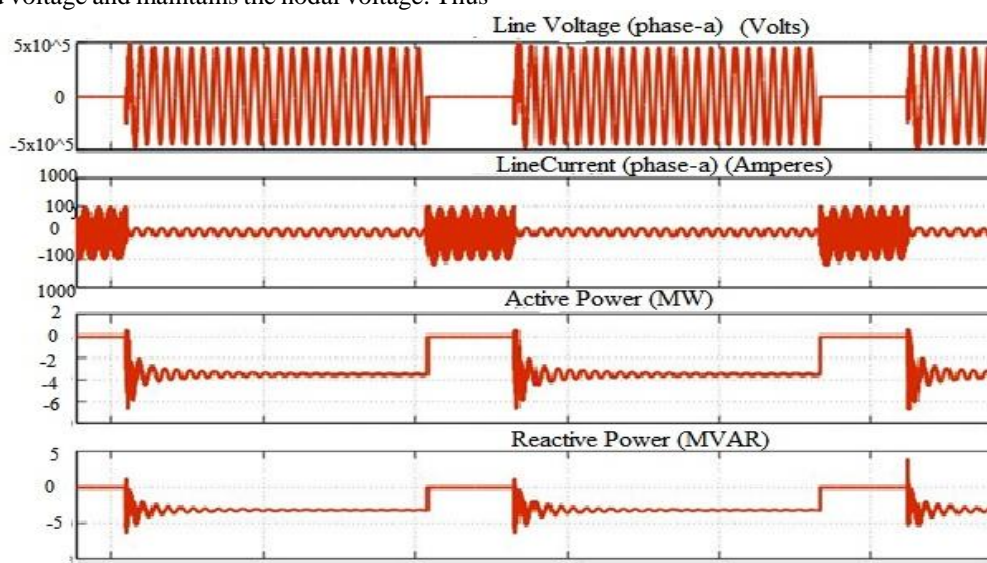


Fig.11. Line Voltage, Line Current, Active Power and Reactive Power of an Uncompensated System

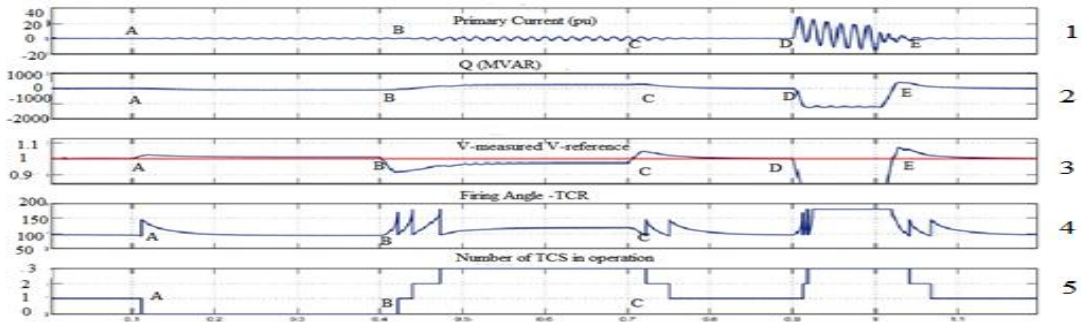


Fig.12. Line Voltage, Line Current, Active Power and Reactive Power of an Uncompensated System

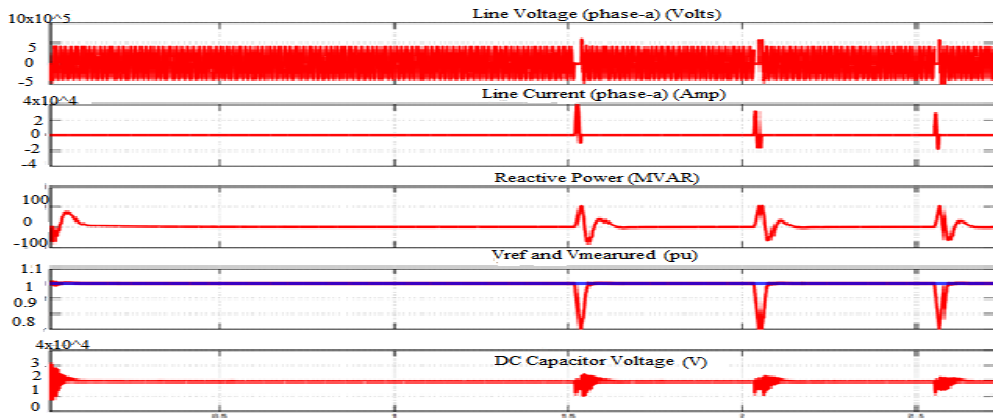


Fig.13 Waveforms of Line V, I, Q, Ref. V and Line V, DC Capacitor V, with STATCOM

The waveforms of the parameters V, I, Q, and number of TSCs included, with SVC in the system are taken from simulation environment to the outside world, and seen on DSO when executed on Real-Time Simulator OPAL-RT OP4510. Instead of signals given to DSO, they can be given to controller, for testing its response for certain conditions. Also the signals from DSO, or say from controller, can be taken from outside world to the simulation environment for its performance evaluation. Similarly, the V, I, Q, and DC Voltage signals are taken out of the simulation environment to the outside world with the STATCOM in the system, and executed on Real-Time Simulator. The signals need to be

scaled down while taking them outside of the simulation environment.

Fig. 14 shows the waveforms of V, I, Q, and number of Thyristor Switched Capacitors (TSC) included in the system, just same as shown in Fig.12. These waveforms are taken out from MATLAB/Simulink environment to outside using Opctrl, AnalogIn, and AnalogOut blocks from OPAL-RT library, and using import/output devices, and seen on DSO. Fig. 15 shows the V, I, Q, and DC capacitor voltage variation with STATCOM implementation. The waveforms discussed in Fig.13 are seen on DSO using the same blocks as used with SVC implementation.

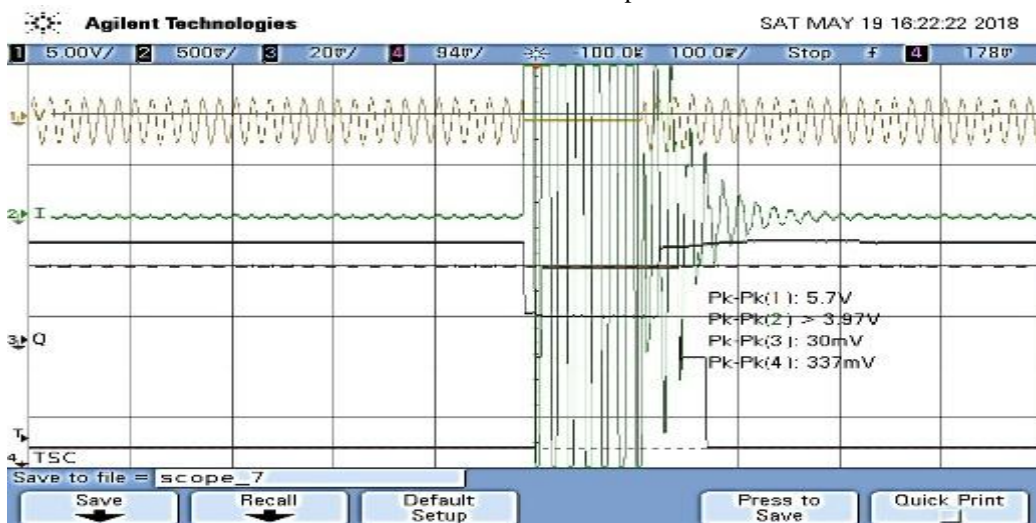


Fig.14 Waveforms of V, I, Q, and Number of TSC in operations on DSO with LLLG fault, during execution with SVC on Real-Time Simulator

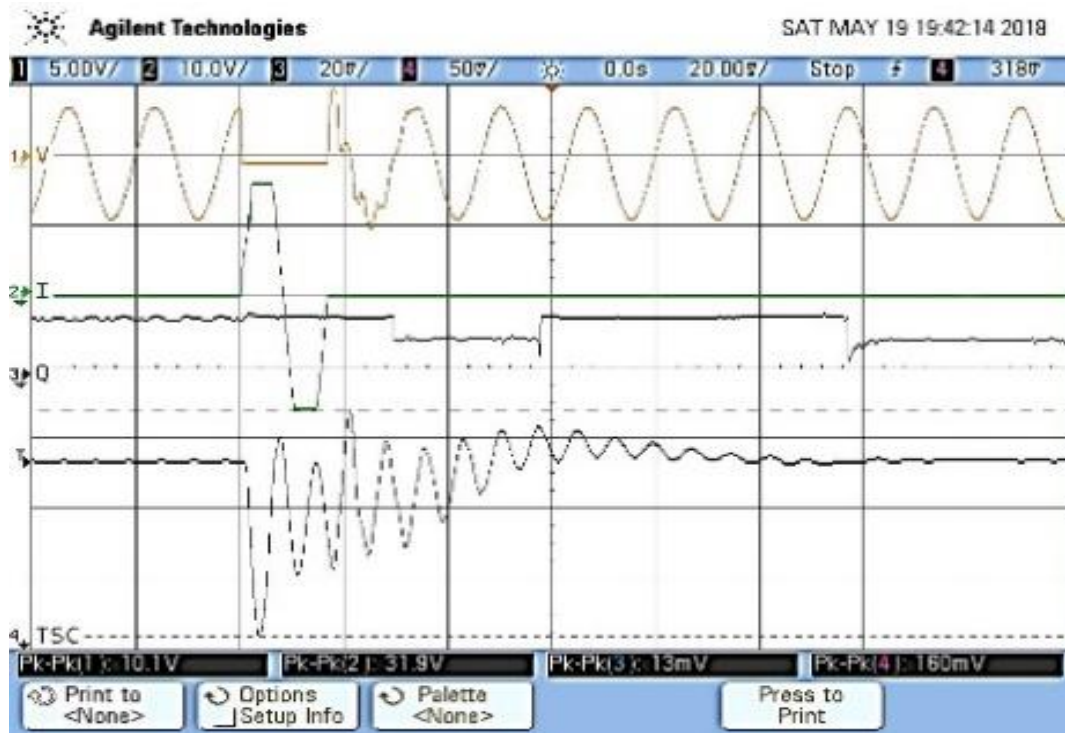


Fig.15. Waveforms of V, I, Q, and DC Capacitor voltage on DSO with LLLG fault during execution with STATCOM, on Real-Time Simulator

V. CONCLUSION

The novel work of implementing SVC, and STATCOM on Multi-machine 9 bus network and computing LFA with and without SVC and STATCOM were performed and with SVC, and STATCOM voltage profile has improved at all the buses, and the total active and reactive power losses have reduced. The real time execution of SVC with fault condition, indicate that it maintains the system voltage magnitude by supplying/absorbing reactive power to/from the system, only if it is within its rated MVAR, during LLLG fault it is unable to maintain system voltage.

Thus it has a limitation of supplying reactive power when the system voltage drops to a low value, whereas STATCOM supplies reactive power even independent of line voltage value. Thus the real-time simulation helps the power system operator to decide appropriate controller to be installed, for specific objectives, while upgrading the transmission line by looking its response with various network conditions.

REFERENCES

1. B. Muruganantham, R. Gnanadass, and N. P. Padhy, "Performance analysis and comparison of load flow methods in a practical distribution system", 2016 National Power Systems Conference (NPSC) (pp. 1-6). IEEE
2. M. O. Faruque, T. Strasser, G. Lauss, V. Jalili-Marandi, P. Forsyth, C. Dufour, C., and Strunz, K "Real-time simulation technologies for power systems design, testing, and analysis", (2015), IEEE Power and Energy Technology Systems Journal, 2(2), 63-73.
3. P. M. Menghal, and A. J. Laxmi, "Real time simulation: Recent progress and challenges", 2012 International Conference on Power, Signals, Controls and Computation (pp. 1-6). IEEE.
4. A. H. Al-Mubarak, M. H. Khan, and M. Z. Al-Kadhem, "Dynamic reactive power compensation for voltage support using static var compensator (SVC) in Saudi Arabia", (2015), IEEE Electrical Power and Energy Conference (EPEC) (pp. 484-490). IEEE
5. V. T. Bui, and D. N. Truong, "Voltage Stability Enhancement of Bac Lieu Wind Power by ANFIS Controlled Static Var Compensator", (2018, November), 4th International Conference on Green Technology and Sustainable Development (GTSD) (pp. 96-99).

6. B. Khan, and M. Kassas, "FSIG-Based Wind Power Plant Transient Stability Margin Improvement, a STATCOM/SVC Comparison", 2019 IEEE Texas Power and Energy Conference (TPEC) (pp. 1-6). IEEE.
7. C. Roy, D. Chatterjee, and T. Bhattacharya, "A Hybrid FACTS Topology for Reactive Power Support in High Voltage Transmission Systems", IECON 2018-44th Annual Conference of the IEEE Industrial Electronics Society (pp. 65-70). IEEE.
8. A. K. Dhulshette, S. Ushkewar, A. A. Khan, H. Rao, and N. R. Ahire, "Validation of STATCOM Capabilities through Modelling And Simulation On Simulink Platform", (2018, February) Fourth International Conference on Advances in Electrical, Electronics, Information, Communication and Bio-Informatics (AEEICB) (pp. 1-5). IEEE.
9. G. Koundal, and S. L. Shimi, "Recent Trends on Real Time Simulation of FACTS: A Review", International Conference on Computational and Characterization Techniques in Engineering and Sciences (CCTES), 2018, September. (pp. 230-235). IEEE.
10. M. Larsson, "ObjectStab-an educational tool for power system stability studies", (2004) IEEE Transactions on Power Systems, 19(1), 56-63.
11. R. Anand, and V. Balaji, "Power flow analysis of Simulink IEEE 57 bus test system model using PSAT", (2015), Indian Journal of Science and Technology, 8(23), 1-9.
12. R. M. Mathur and R. K. Varma, "Thyristor-based FACTS controllers for electrical transmission systems", (2002), John Wiley and Sons.
13. E. Acha, C. R. Fuerte-Esquivel, H. Ambriz-Perez, and C. Angeles-Camacho, "FACTS: modelling and simulation in power networks", (2004), John Wiley and Sons.
14. N. G. Hingorani, L. Gyugyi, and M. El-Hawary, (2000). Understanding FACTS: concepts and technology of flexible AC transmission systems (Vol. 1). New York: IEEE press.
15. B. K. Medhi and S. Bhuyan, "Performance analysis of some FACTS devices using Newton Raphson Load Flow algorithm", (2014, February). First International Conference on Automation, Control, Energy and Systems (ACES) (pp. 1-6). IEEE.
16. OPAL-RT-4510 User Manual and RT-LAB Block Library Reference Guide.

AUTHORS PROFILE



Anjali A. Bhandakkar is Lecturer in Electrical Engineering Department, in Government Polytechnic, Pen, in Maharashtra. She has more than 25 years of teaching experience. She is pursuing PhD in the National Institute of Technical Teacher's Training Institute, Chandigarh, under the guidance of Dr. Lini Mathew. She has published 4 papers in conferences. She is life time member of ISTE and Institution of Engineers (India). Her main areas of interest are Power System, Power Electronics, and Control System.



Dr. Lini Mathew is presently working as Professor in the Electrical Engineering Department of National Institute of Technical Teachers Training and Research, Chandigarh, India. She holds a Bachelor degree in Electrical Engineering from Kerala University, and Masters and Ph.D from Panjab University. She has 34 years of experience out of which 2 years are of industrial and the rest of teaching. She has guided more than 100 Master's degree theses and 2 doctoral theses. 7 doctoral theses are in the pipeline. She has published more than 150 papers in National and International Journals and Conferences. Her areas of specialization are Power Systems, Soft Computing Techniques, Virtual Instrumentation, Biomedical Instrumentation etc.